Acta Cryst. (1996). B52, 159–164

Electron-Density Study of *m*-Nitrophenol in the Orthorhombic Structure

F. HAMZAOUI,[a] F. BAERT[a] AND G. WOJCIK[b]

[a]*Laboratoire de dynamique et structure des matériaux moléculaires, associé au CNRS URA 801, Université des sciences et Technologies de Lille, 59655 Villeneuve d'Ascq CEDEX, France, and* [b]*Institute of Organic and Physical Chemistry, Technical University of Wrocław, 50-370 Wyb, Wyspianskiego 27, Poland*

(*Received 20 January 1995; accepted 19 May 1995*)

Abstract

m-Nitrophenol (*m*-NPH) occurs at room temperature in two solid modifications: monoclinic $P2_1/n$ and orthorhombic $P2_12_12_1$ [Pandarese, Ungaretti & Coda (1975). *Acta Cryst.* B31, 2671–2675]. The thermal vibrations and electronic-density distribution of the molecule in the orthorhombic structure have been analyzed in terms of Stewart's rigid pseudoatom model, using restricted Slater radial functions and angular multipole terms extending to actapoles for C, N and O and dipoles for H pseudoatoms. The net atomic charge and the in-crystal molecular dipole moment have been determined in order to understand the nature of the inter- and intramolecular charge transfer. The analysis suggests that aspherical pseudoatoms are essential for modeling the charge distribution in a noncentrosymmetric crystal. Careful consideration must also be given to the treatment of the H atoms, in the absence of complementary neutron diffraction data.

1. Experimental

The purification of the material and the crystal growing were published earlier (Wojcik & Marqueton, 1989) and the experimental details and crystal data are given in Table 1.

X-ray intensity data were measured on a CAD-4 diffractometer using graphite-monochromated Mo$K\alpha$ radiation (50 kV, 35 mA). A crystal of high quality was cooled by a stream of cold nitrogen gas. Lattice constants were determinated by a least-squares fit of setting angles for 25 well centered reflections in the range $11 \leq \theta \leq 25°$. The profiles of the different reflections were measured using the θ–2θ step scan method. Three standard reflections were measured every 2 h, the corresponding linear decay correction was performed but nonsignificant variation was observed and the obtained instrumental factor was 0.015. The intensities were measured only once with a relatively slow speed of $1.02° \text{ min}^{-1}$. A total of 2224 intensities were collected and merged to give 2004 independent reflections. The internal agreement for all equivalent reflections was 0.02 (in reality only the standard references were measured more times). As a preliminary check on the X-ray intensity data, the atomic positions were obtained by a redetermination of the structure with the *SHELXS* (Sheldrick, 1976) program, for comparison with the published (room-temperature) crystal structure (Wojcik & Toupet, 1993). H atoms were located in a difference map and adjusted to their theoretical position. The reflection profiles were analyzed as described by Blessing (1989), and references therein.

Table 1. *Experimental details*

Crystal data	
Chemical formula	$C_6H_5NO_3$
Chemical formula weight	139.11
Cell setting	Orthorhombic
Space group	$P2_12_12_1$
a (Å)	11.136 (2)
b (Å)	6.649 (1)
c (Å)	8.091 (1)
V (Å^3)	598.7
Z	4
D_x (Mg m^{-3})	1.54
Radiation type	Mo $K\alpha$
Wavelength (Å)	0.71073
No. of reflections for cell parameters	25
θ range (°)	11–25
μ (mm^{-1})	0.118
Temperature (K)	122 (1)
Crystal color	Colorless
Data collection	
Diffractometer	Nonius CAD-4
Data collection method	θ–2θ
Absorption correction	None
No. of measured reflections	2224
No. of independent reflections	2004
No. of observed reflections	1573
Criterion for observed reflections	$I > 3\sigma(I)$
R_{int}	0.02
Range of h, k, l	$0 \rightarrow h \rightarrow 26$ $0 \rightarrow k \rightarrow 13$ $0 \rightarrow l \rightarrow 15$
No. of standard reflections	3
Frequency of standard reflections	120
Refinement	
Refinement on	F^2
$R[F^2 > 2\sigma(F^2)]$	0.027
$wR(F^2)$	0.038
S	1.20
No. of reflections used in refinement	1573
No. of parameters used	221
Weighting scheme	$w = 1/\sigma^2(I)$
Extinction method	None
Source of atomic scattering factors	*International Tables for X-ray Crystallography* (1974, Vol. IV)

1.1. *Least-squares refinement*

Since there were only 477 data with $s = \sin(\theta/\lambda) \geq 0.8\,\text{Å}^{-1}$ and $I/\sigma(I) \geq 3$, a high-angle refinement of the non-H atoms was made against 960 data with $s \geq 0.6\,\text{Å}^{-1}$ using the program *LINEX* (Becker & Coppens, 1974); this refinement was based on F^2 with weights calculated as $w = 1/\sigma^2(I)$. The H atoms were found by difference-Fourier synthesis and their coordinates were adjusted by extending along the C—H and O—H bond directions to bond lengths of 1.085 and 0.96 Å, respectively. The X-ray scattering factors for C, N and O atoms were taken from the *International Tables for X-ray Crystallography* (1974, Vol. IV), while for H the bonded H-atom scattering curve of Stewart, Davidson & Simpson (1965) was used.

As the structure is noncentrosymmetric, it is necessary to have very accurate phases for the structure factors in order to obtain reliable electron-density maps and derive correct molecular properties. Then, the multipolar atomic electron-density model of Hansen & Coppens (1978) was used to analyze the electron charge density. The electron densities at each atom are described by

$$\rho_i = P_{i,c}\rho_{i,c} + P_{i,v}\kappa_i'^3\rho_{i,v}(\kappa_i r_i) + \sum_{l=0}^{4}\kappa_i''^3 R_l(\kappa_i''^3 r_i)\sum_{m=-l}^{l} P_{lm}Y_{lm}(\mathbf{r}/r),$$

where ρ_c and ρ_v are spherically averaged Hartree–Fock core and valence densities, with ρ_v normalized to one electron, Y_{lm} are multipolar spherical harmonic angular functions in real form and $R_l = N_l r^n \exp(-\kappa'\xi r)$ are Slater-type radial functions with N_l as a normalization factor and $n = n(l)$ and ξ are parameters chosen according to the criteria given by Hansen & Coppens (1978).

The multipole refinement was carried out with the program *MOLLY* (Hansen & Coppens, 1978). The development was trunked to the third-order $l_{max} = 3$ and the coefficients of the hexadecapole functions ($l = 4$) constrained to be zero. The coefficients of the radial function were $n_1 = 2,2$ and 3 (for $l = 1,2,3$, respectively) for non-H atoms, and $n_1 = l$ for H. The core and valence scattering factors were taken from *International Tables for X-ray Crystallography* (1974, Vol. IV). The total charge of the unit cell was constrained to be neutral. The positional, thermal, multipole and radial (κ) parameters of non-H atoms were refined based on 1573 reflections with $I \geq 3\sigma(I)$. The κ refinement was also carried out to estimate the effective charge of the different atoms of the molecule, see Table 6. Selected results of the multipolar refinement are presented in Table 7.*

*A list of structure factors has been deposited with the IUCr (Reference: PA0307). Copies may be obtained through The Managing Editor, International Union of Crystallography, 5 Abbey Square, Chester CH1 2HU, England.

Table 2. *Fractional atomic coordinates and equivalent isotropic displacement parameters (Å²)*

$U_{eq} = (1/3)\Sigma_i\Sigma_j U_{ij} a_i^* a_j^* \mathbf{a}_i.\mathbf{a}_j.$

	x	*y*	*z*	B_{eq}
C1	0.6281 (1)	0.1561 (2)	0.8943 (2)	11 (1)
C2	0.5623 (1)	0.0756 (2)	0.7647 (1)	11 (1)
C3	0.6016 (1)	0.1133 (2)	0.6042 (1)	12 (1)
C4	0.7040 (1)	0.2314 (2)	0.5777 (2)	14 (1)
C5	0.7673 (1)	0.3101 (3)	0.7116 (2)	14 (1)
C6	0.7303 (1)	0.2727 (2)	0.8729 (2)	12 (1)
N	0.5861 (1)	0.1168 (2)	1.0623 (1)	14 (1)
O1	0.6434 (1)	0.1885 (2)	1.1783 (1)	17 (2)
O2	0.4969 (1)	0.0111 (3)	1.0816 (2)	20 (1)
O	0.5371 (1)	0.0334 (2)	0.4787 (1)	15 (1)
HO	0.5673	0.0824	0.3749	222

Table 3. *Anisotropic thermal parameters ($\times 10^4$ Å²)*

(*A* and *B* correspond, respectively, to the multipolar and high-order refinements).

	U_{11}	U_{22}	U_{33}	U_{23}	U_{13}	U_{12}
C1*A*	140 (2)	132 (3)	84 (2)	−2 (2)	3 (2)	−2 (2)
C1*B*	139 (4)	132 (5)	85 (4)	2 (3)	1 (3)	0 (3)
C2*A*	147 (3)	141 (3)	92 (2)	−25 (2)	4 (2)	−1 (2)
C2*B*	145 (4)	144 (6)	94 (4)	−23 (3)	2 (3)	−4 (3)
C3*A*	148 (3)	141 (3)	89 (2)	−9 (2)	0 (2)	−2 (2)
C3*B*	143 (4)	143 (5)	95 (4)	−3 (3)	−2 (3)	−1 (3)
C4*A*	150 (2)	170 (3)	109 (2)	−15 (2)	15 (2)	13 (2)
C4*B*	154 (4)	164 (5)	108 (5)	−14 (4)	14 (3)	12 (3)
C5*A*	145 (3)	188 (3)	131 (2)	−44 (3)	5 (2)	9 (2)
C5*B*	146 (4)	178 (6)	140 (5)	−36 (4)	2 (3)	8 (4)
C6*A*	146 (2)	168 (3)	119 (2)	−30 (2)	−12 (2)	−7 (2)
C6*B*	151 (4)	162 (5)	118 (4)	−28 (4)	−12 (3)	−7 (3)
N*A*	175 (2)	146 (3)	97 (2)	6 (2)	8 (2)	−2 (2)
N*B*	175 (5)	143 (5)	91 (4)	13 (3)	7 (3)	0 (3)
O1*A*	276 (2)	243 (3)	87 (2)	−43 (2)	−12 (2)	−16 (2)
O1*B*	266 (6)	237 (6)	93 (4)	−40 (4)	−21 (4)	−19 (3)
O2*A*	223 (2)	287 (3)	141 (2)	−84 (2)	46 (2)	5 (2)
O2*B*	218 (5)	285 (7)	141 (4)	−79 (4)	48 (4)	5 (4)
O*A*	217 (2)	229 (3)	87 (2)	−57 (2)	−13 (2)	−9 (2)
O*B*	218 (5)	224 (6)	94 (4)	−57 (4)	−18 (3)	−14 (3)

2. Discussion

2.1. *The structural analysis*

The structural analysis has already been treated in detail in earlier works (Wojcik & Toupet, 1993). The main characteristic of this structure is that the four molecules in the unit cell are engaged in four chains realized by infinite chains of hydrogen-bonded coplanar molecules. The different chains link translationally equivalent molecules along the *c* crystallographic axis through O—H and NO_2. The O—H···O(1) distance is 1.94 Å and the O—H···O angle is *ca* 174° (see Table 4).

2.2. *Thermal vibration analysis*

The rigid-bond test (Hirshfeld, 1976) led to some large values of mean-square displacement amplitudes (MSDA's) along the nonbonded intramolecular interatomic directions, indicating that the molecule is not entirely rigid and that low-frequency soft modes of internal molecular vibration contribute significantly to the observed mean-square displacements (Rosenfield, Trueblood & Dunitz, 1978).

Table 4. *Bond lengths (Å) and angles (°) with e.s.d.'s in parentheses*

C1—C2	1.387 (1)	C4—C5	1.393 (1)
C1—C6	1.386 (1)	C4—H4	1.083 (1)
C1—N	1.462 (1)	C5—C6	1.391 (1)
C2—C3	1.393 (1)	C5—H5	1.084 (1)
C2—H2	1.084 (1)	C6—H6	1.083 (1)
C3—C4	1.399 (1)	N—O1	1.233 (1)
C3—O	1.352 (1)	N—O2	1.225 (1)
		O—HO	0.963 (1)
C6—C1—N	118.6 (1)	C5—C4—H4	119.7 (1)
C2—C1—N	117.6 (1)	C4—C5—C6	120.9 (1)
C2—C1—C6	123.8 (1)	C4—C5—H5	119.9 (1)
C1—C2—H2	120.1 (1)	C6—C5—H5	119.1 (1)
C1—C2—C3	117.8 (1)	C1—C6—C5	117.2 (1)
C3—C2—H2	122.1 (1)	C1—C6—H6	122.7 (1)
C2—C3—O	117.3 (1)	C5—C6—H6	120.0 (1)
C2—C3—C4	120.0 (1)	C1—N—O1	118.4 (1)
C4—C3—O	122.6 (1)	C1—N—O2	118.9 (1)
C3—C4—H4	120.1 (1)	O1—N—O2	122.8 (1)
C3—C4—C5	120.2 (1)	C3—O—HO	109.6 (1)
C6—C1—N—O1	0.29 (10)	H2—C2—C3—C4	179.49 (10)
C6—C1—N—O2	−178.78 (10)	C1—C2—C3—C4	−0.62 (10)
C2—C1—N—O1	−179.30 (10)	C4—C3—O—HO	−6.14 (10)
C2—C1—N—O2	1.63 (10)	C2—C3—C4—C5	0.38 (10)
C6—C1—C2—C3	0.24 (10)	H4—C4—C5—C6	−179.77 (10)
C6—C1—C2—H2	−179.87 (10)	C3—C4—C5—C6	0.26 (10)
N—C1—C6—C5	−179.18 (10)	C4—C5—C6—C1	−0.63 (10)
		H5—C5—C6—C1	179.44 (10)

Table 5. *Matrix for differences in MSDA's and anisotropic H-atom parameters ($Å^2 \times 10^4$)*

(*a*) Values listed are 10^4 MSDA's for column atom minus that for row atom, underlined values correspond to chemical bonds.

	O	O1	O2	N	C6	C5	C4	C3	C2
C1	−4	3	0	14	−5	1	10	5	1
C2	−10	25	−7	6	−4	−5	2	2	
C3	−2	22	−6	7	1	−5	−1		
C4	−2	10	−8	4	−2	−7			
C5	4	1	−1	6	4				
C6	−3	−10	−5	1					
N	−16	−14	−8						
O1	−2	−4							
O2	−42								

Inertial moments	164	483	648
Libration axis	C1—N		
$\langle(\varphi+2\varphi)(\varphi+2\varphi_\parallel)\rangle$ (deg^2)	33 ± 7		
Force constant (J mol^{-1} deg^2)	33.9		
Libration tensor **L** (deg^2)	9.580	−0.935	0.327
		2.022	−0.054
			3.169

$R = [\sum w(u_{calc} - u_{obs})^2 / \sum u_{obs}^2]^{1/2} = 0.045$.
R.m.s. $= [\sum(w(u_{obs} - u_{calc}))^2 / \sum w^2]^{1/2} = 0.0005$.

(*b*) Anisotropic parameters from TLS + φ + internal vibrations

	U_{11}	U_{22}	U_{33}	U_{12}	U_{13}	U_{23}
H2	262	306	364	−102	22	33
H4	378	383	197	27	62	85
H5	269	412	431	−142	38	34
H6	351	390	277	−53	73	−109
HO	261	269	136	−30	19	−28

The MSDA's were modeled by fitting molecular **T**, **L** and **S** plus correlated φ_i tensors to the atomic **U** tensors. The **T**, **L** and **S** model the external lattice vibrations of the whole molecule and the φ_i model low-frequency large-amplitude internal molecular vibrations as librations of rigid groups of atoms within the flexible molecule (Dunitz, Schomaker & Trueblood, 1988). The **TLS** + Φ_i analyses were carried out using the *THMA*11 program of Trueblood (1990), which includes a six-parameter model for the physical correlations between each internal torsional mode and the external lattice mode. The average MSDA for bond pairs is 5.55×10^{-4} Å, so the displacement parameters fit the rigid bond criterion well; the details of this refinement are listed in Table 5(*a*).

The thermal parameters for the H atoms were approximated as consisting of a rigid molecular motion plus internal C—H vibrations. The total vibration tension for each H atom is then obtained by algebraic summation of these two contributions (Baert, Schweiss, Heger & More, 1988). For the H atoms of the phenyl ring, the frequencies led to estimated MSDA's of 0.0056, 0.014 and 0.25 Å^2 for bond stretching, in-plane bending and out-of-plane bending, respectively, while for the H atom of the hydroxyl group implied in a hydrogen bond with an adjacent molecule, values of 0.05, 0.025 and 0.012 Å^2 were respectively applied to the different types of internal vibrations. The thermal parameters of the H atoms calculated in this way are listed in Table 5(*b*). The ellipsoids of the different atoms representing their thermal motion described above are presented with an *ORTEP* (Johnson, 1976) diagram in Fig. 1.

2.3. *Electron-density maps*

For noncentrosymmetric structures, reliable deformation maps require two sets of structure amplitudes and two sets of phases (Souhassou, Lecomte, Blessing, Aubry, Rohmer, Wiest, Bénard & Marraud, 1991). The crystallographic deformation-density maps were calcu-

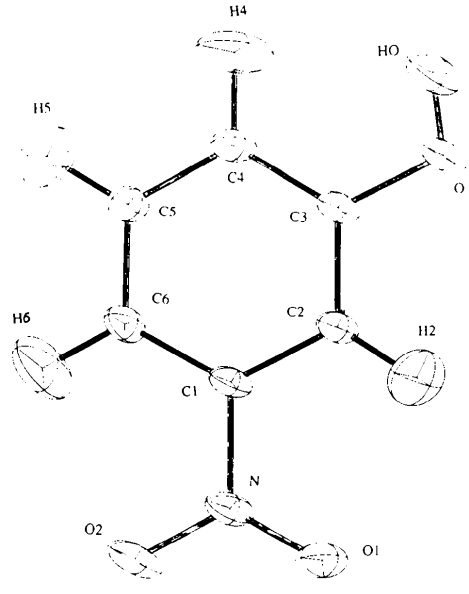

Fig. 1. *ORTEP*II (Johnson, 1976) diagram of the *m*-nitrophenol molecule; thermal ellipsoids are at the 30% level.

lated according to

$$\Delta\rho(r) = V^{-1}\sum_h [|F_m(h)|e^{i\varphi_m(h)} - |F_s(h)e^{i\varphi_s(h)}|]e^{-2i\pi\mathbf{hr}},$$

where the subscript m refers to quantities calculated from the multipolar model and s refers to quantities determined from a model with neutral spherical atoms. In the reference cited above the authors have shown that the introduction of the phase correction can increase the total charge density by *ca* 25% in the monoclinic structures. In the orthorhombic structures the influence is not so important but it is not negligible, for some peaks the

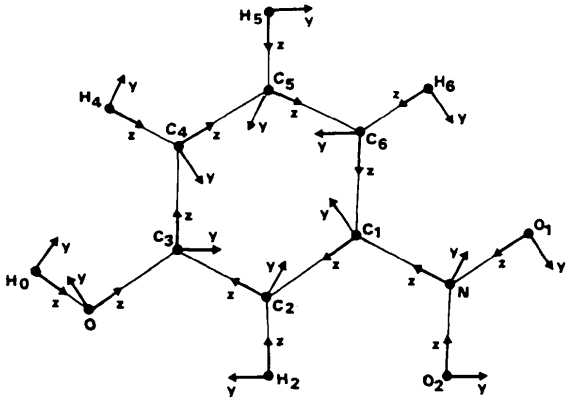

Fig. 2. Labeling of the atoms and definition of local orthogonal reference axes for the atom-centered multipolar functions.

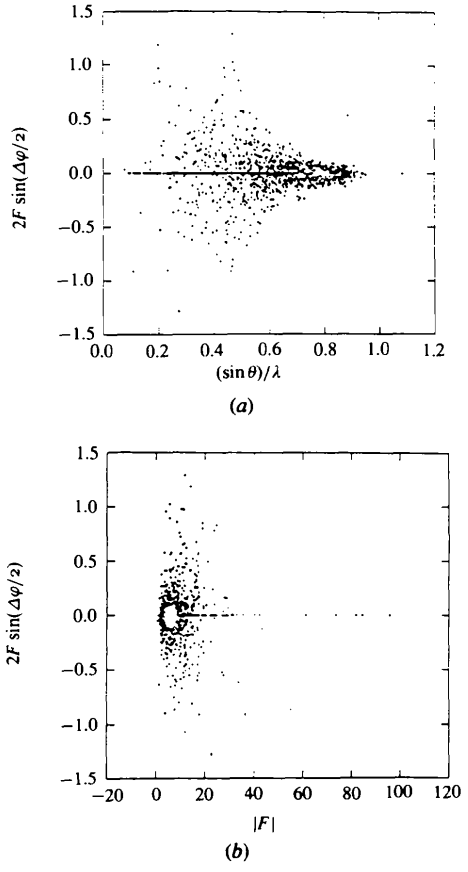

Fig. 3. Distribution of $2F\sin(\Delta\varphi/2)$ against (*a*) $(\sin\theta)/\lambda$ and (*b*) $(|F|)$.

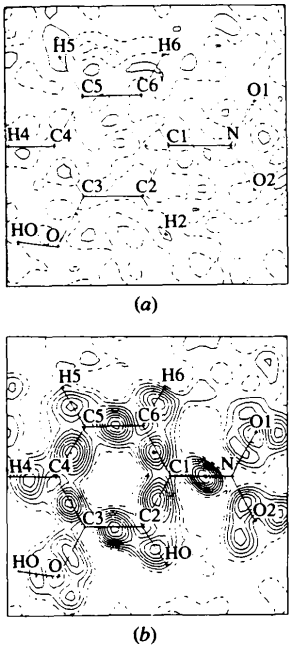

Fig. 4. (*a*) Residual density in the phenyl ring; contours as in Fig. 4. (*b*) Experimental density maps in the phenyl ring calculated from the high-order refinement; contour interval 0.05 e Å^{-3}.

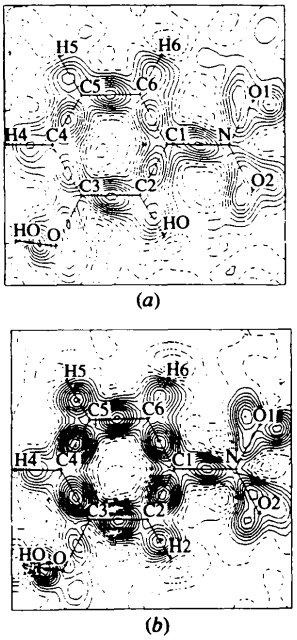

Fig. 5. Multipole deformation-density maps calculated in the phenyl ring; contour interval 0.05 e Å^{-3}. (*a*) Without phase correction; (*b*) with phases derived from multipolar refinement.

density difference can achieve 15%. Fig. 4 shows the electron-density maps in the phenyl plane with and without the phase corrections. In order to illustrate the reflection types which are more affected by the phase problem, we have represented in Fig. 3 the distribution of $2|F|\sin(\Delta\varphi/2)$ as a function of $(\sin\theta)/\lambda$ and $|F|$. Fig. 3(*a*) clearly shows the importance of the phase correction for the low-order reflections. It is also apparent in Fig. 3(*b*) that the weak and medium-to-weak reflections have an important influence. Consequently, the measurement and the processing of the low-angle weak reflections deserve special care. An experimental map from the high-order refinement is also given in Fig. 5(*b*); by comparison to Fig. 4(*b*), one can observe that the introduction of the multipolar phases has more effect in centering well the density peaks along the different bonds and localizing well the lone pairs of the O atoms. The residual map given in Fig. 5(*a*) shows the adequacy of the multipolar model to describe the experimental density of the *m*-nitrophenol molecule.

2.4. *The hydrogen bond*

In the deformation-density maps there are $-0.2\,e\,Å^{-3}$ minima near the H atoms opposite the C—H and O—H bonds. The H atoms were positioned to give 1.085 and 0.96 Å C—H and O—H bond lengths, respectively. Any errors in the H-atom position will produce strongly correlated errors in the hydrogen dipole populations. These correlations are probably largely responsible for the experimental minima near the H atoms, which may indicate that the chosen C—H and O—H bond lengths were a little too long.

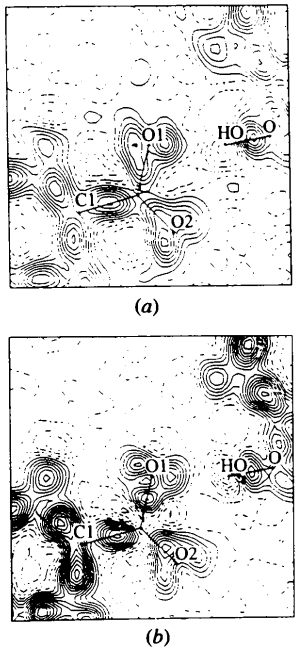

Fig. 6. Deformation-density maps in the plane of the hydrogen bond; (*a*) without phase correction; (*b*) with phases derived from multipolar refinement. Contours as in Fig. 4.

Table 6. *Net atomic charge in m-nitrophenol and magnitude of the molecular dipole moment*

A Kappa refinement; *B* multipolar refinement; *C* semi-empirical calculation using *MOPAC* (Stewart, 1990)

	A	*B*	*C*
C1	+0.060 (4)	−0.035 (8)	−0.130
C2	−0.395 (1)	−0.246 (7)	−0.050
C3	+0.363 (3)	+0.046 (5)	+0.370
C4	−0.279 (2)	−0.000 (8)	−0.110
C5	−0.207 (5)	−0.353 (6)	+0.050
C6	−0.162 (4)	−0.095 (2)	+0.004
N	+0.325 (2)	+0.440 (9)	+1.090
O1	−0.289 (4)	−0.270 (4)	−0.580
O2	−0.313 (3)	−0.280 (5)	−0.580
O	−0.573 (4)	−0.410 (10)	−0.480
H2	+0.340 (3)	+0.260 (4)	+0.060
H4	+0.214 (3)	+0.140 (3)	+0.020
H5	+0.240 (4)	+0.230 (2)	+0.003
H6	+0.230 (2)	+0.170 (3)	+0.040
HO	+0.454 (2)	+0.380 (5)	+0.250
Molecular dipole moment			
$\|\mu\|$ (Debye)	7.58 (22)	5.28 (31)	6.24

Fig. 6 shows the experimental deformation density in the plane of the intermolecular hydrogen bond. The figure shows that the two O1 lone pairs are located in the plane of the hydrogen bond. A significant $-0.30\,e\,Å^{-3}$ minimum occurs close to the H atom, between it and O1, which is consistent with an electrostatic description of hydrogen bonding.

2.5. *The molecular dipole moment*

The valence population coefficients P_v^i were used to estimate the partial charges on the different atoms according to the equation

$$q_i = n_i - P_v^i,$$

where n_i is the total number of electrons of atom i. The results obtained by the kappa and multipolar refinement are summarized in Table 6(*a*), which also gives the same values derived from the semiempirical calculations using the *MOPAC* program (Stewart, 1990). All the methods are in agreement for the evaluation of the positive sign of the net charges on the H atoms and the negative net charges on the O atoms. The semiempirical values appear somewhat larger than the experimental charges, which can be explained by the absence of the thermal vibration effects in the semiempirical calculations.

The molecular dipole moment was calculated from the monopole and dipole population parameters and the radial exponents, following the procedure described by Hansen & Coppens (1978), and the results are compared with those obtained by semiempirical calculation using the *MOPAC*6 program, see Table 6(*b*). The orientations for these molecular dipole moments are shown in Fig. 7. The general conclusion from these estimates of the dipole moment is that the region of the nitro and hydroxyl

Table 7. *Selected results of multipolar refinement*

(*a*) Local site symmetry and deformation types *imposed* on the atoms of the molecule and values of the expansion–contraction parameters found by the multipolar refinement.

Atoms	Deformation type	Local site symmetry	κ'	κ''
C1	1	*m*	1.02	1.05
C2	2	*m*	0.99	1.10
C3	3	*m*	1.02	1.09
C4	4	*m*	1.01	1.02
C5	5	*m*	1.00	1.29
C6	6	*m*	1.01	1.06
N	7	*m*	1.02	0.70
O1, O2	8	*m*	1.01	1.11
O	9	*m*	0.96	1.02
H atoms	10	C_∞	1.07	1.81

(*b*) The population parameters are normalized according to Hansen & Coppens (1978). The symmetry imposed on the molecule (Fig. 7) requires that $d_1 = q_2 = q_5 = o_2 = o_5 = o_6 = 0$ for all non-H atoms, and for the H atoms only P_V and d_3 are not equal to zero. (P_V is the valence population coefficient; d_i, q_i and o_i are the dipole, quadrupole and octapole population coefficients, respectively, of the *i* atom.)

	P_V	d_2	d_3	q_1	q_3	q_4	o_1	o_3	o_4	o_7
C1	4.035	0.044	0.016	0.1210	−0.0420	−0.1090	0.2260	−0.0040	0.2030	−0.0300
C2	4.246	−0.043	0.013	0.1330	0.0090	−0.1910	0.2130	−0.0080	0.2030	−0.0160
C3	3.954	0.046	0.121	0.1230	−0.0810	−0.1500	0.1990	0.0490	0.2080	−0.0550
C4	3.977	−0.011	0.012	0.1430	−0.0180	−0.1660	0.2430	0.0290	0.1880	0.0090
C5	4.353	−0.026	−0.023	0.1120	0.0030	−0.1930	0.1670	0.0030	0.1800	−0.0160
C6	4.095	−0.037	−0.014	0.1370	−0.0310	−0.1570	0.2280	0.0230	0.1490	−0.0010
N	4.566	−0.011	0.035	0.0630	0.0040	−0.1060	0.2120	−0.440	0.1690	−0.0050
O1	6.270	−0.003	0.030	−0.0410	−0.0280	−0.1650	0.0660	−0.0040	0.0290	0.0140
O2	6.281	−0.000	0.038	0.0050	0.0090	−0.1350	0.0340	0.0550	0.0170	0.0510
O	6.411	−0.011	−0.066	−0.0670	−0.0670	−0.0570	0.0950	−0.0480	0.0680	0.0700
H2	0.744	—	0.086							
H4	0.865	—	0.102							
H5	0.777	—	0.068							
H6	0.835	—	0.122							
HO	0.626	—	0.061							

groups is electronegative and the region of the C—H groups is electropositive.

In a parallel study, we are working on the determination of the electron density of the monoclinic compound. The knowledge of the electrostatic potential created around the molecule in both the orthorhombic and the monoclinic structures will lead to some explanations about the existence of the polymorphism in *m*-nitrophenol compounds.

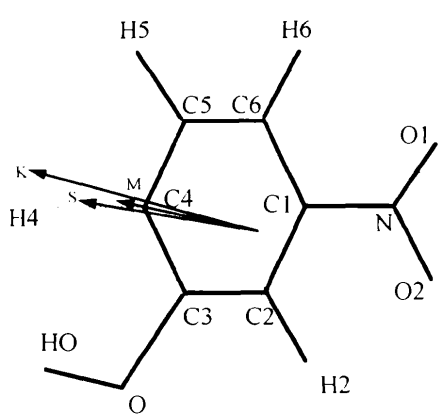

Fig. 7. Molecular dipole moment calculated by different methods. The origin is at the center of mass of the molecule. S = Molecular dipole moment from semiempirical calculation; M = molecular dipole moment from multipolar refinement; K = molecular dipole moment from κ refinement.

References

Baert, F., Schweiss, P., Heger, G. & More, M. (1988). *J. Mol. Struct.* **178**, 29–48.

Becker, P. & Coppens, P. (1974). *Acta Cryst.* A**30**, 129–147.

Blessing, R. H. (1989). *J. Appl. Cryst.* **22**, 396–397.

Dunitz, J. D., Schomaker, V. & Trueblood, K. N. (1988). *J. Phys. Chem.* **92**, 856–867.

Hansen, N. & Coppens, P. (1978). *Acta Cryst.* A**34**, 909–921.

Hirshfeld, F. L. (1976). *Acta Cryst.* A**32**, 239–244.

Johnson, C. K. (1976). *ORTEP*II. Report ORNL-5738. Oak Ridge National Laboratory, Tennessee, USA.

Pandarese, F., Ungaretti, L. & Coda, A. (1975). *Acta Cryst.* B**31**, 2671–2675.

Rosenfield, R. E., Trueblood, K. N. & Dunitz, J. D. (1978). *Acta Cryst.* A**34**, 828–829.

Sheldrick, G. M. (1976). *SHELXS. Program for Crystal Structure Determination.* University of Cambridge, England.

Souhassou, M., Lecomte, C., Blessing, R. H., Aubry, A., Rohmer, M. M., Wiest, R., Bénard, M. & Marraud, M. (1991). *Acta Cryst.* B**47**, 253–266.

Stewart, J. J. P. (1990). *MOPAC Program*, Version. 6.00 (MVS version), QCPE#455 QCPE. Quantium Chemistry Program Exchange.

Stewart, R. F., Davidson, E. R. & Simpson, W. T. (1965). *Chem. Phys.* **42**, 3175–3187.

Trueblood, K. N. (1990). *THMA*11. *Program for Thermal Motion Analysis.* University of California, Los Angeles, USA.

Wojcik, G. & Marqueton, Y. (1989). *Mol. Cryst. Liq. Cryst.* **168**, 247–254.

Wojcik, G. & Toupet, L. (1993). *Mol. Cryst. Liq. Cryst.* **229**, 153–159.